

On the stability of a quasicrystal and its crystalline approximant in a system of hard disks with a soft corona

Harini Pattabhiraman, Anjan P. Gantapara, and Marjolein Dijkstra

Citation: *The Journal of Chemical Physics* **143**, 164905 (2015); doi: 10.1063/1.4934499

View online: <http://dx.doi.org/10.1063/1.4934499>

View Table of Contents: <http://scitation.aip.org/content/aip/journal/jcp/143/16?ver=pdfcov>

Published by the [AIP Publishing](#)

Articles you may be interested in

[Self-consistent phonon theory of the crystallization and elasticity of attractive hard spheres](#)

J. Chem. Phys. **138**, 084510 (2013); 10.1063/1.4792440

[Phase diagram of hard tetrahedra](#)

J. Chem. Phys. **135**, 194101 (2011); 10.1063/1.3651370

[Phase behavior of hard colloidal platelets using free energy calculations](#)

J. Chem. Phys. **134**, 094501 (2011); 10.1063/1.3552951

[Computational study of the melting-freezing transition in the quantum hard-sphere system for intermediate densities. I. Thermodynamic results](#)

J. Chem. Phys. **126**, 164508 (2007); 10.1063/1.2718523

[Phase behavior of hard-core lattice gases: A fundamental measure approach](#)

J. Chem. Phys. **119**, 10832 (2003); 10.1063/1.1615511



AIP | APL Photonics

APL Photonics is pleased to announce
Benjamin Eggleton as its Editor-in-Chief



On the stability of a quasicrystal and its crystalline approximant in a system of hard disks with a soft corona

Harini Pattabhiraman,^{a)} Anjan P. Gantapara, and Marjolein Dijkstra^{b)}

Soft Condensed Matter, Debye Institute for Nanomaterials Science, Department of Physics, Utrecht University, Princetonplein 5, 3584 CC Utrecht, The Netherlands

(Received 9 July 2015; accepted 30 September 2015; published online 27 October 2015)

Using computer simulations, we study the phase behavior of a model system of colloidal hard disks with a diameter σ and a soft corona of width 1.4σ . The particles interact with a hard core and a repulsive square-shoulder potential. We calculate the free energy of the random-tiling quasicrystal and its crystalline approximants using the Frenkel-Ladd method. We explicitly account for the configurational entropy associated with the number of distinct configurations of the random-tiling quasicrystal. We map out the phase diagram and find that the random tiling dodecagonal quasicrystal is stabilised by entropy at finite temperatures with respect to the crystalline approximants that we considered, and its stability region seems to extend to zero temperature as the energies of the defect-free quasicrystal and the crystalline approximants are equal within our statistical accuracy. © 2015 AIP Publishing LLC. [<http://dx.doi.org/10.1063/1.4934499>]

I. INTRODUCTION

Quasicrystals (QCs) are materials that exhibit long-range order but no translational periodicity. The first observation of a metastable quasicrystal was reported by Shechtman and Blech in a rapidly cooled Al-Mn alloy.¹ Since then, quasicrystals have been observed in a wide range of intermetallic alloys. Surprisingly, quasicrystalline order has also been discovered recently in several soft-matter systems, ranging from spherical dendrite micelles,² block copolymers^{3–7} to binary mixtures of nanoparticles.^{8,9} In addition, soft-matter quasicrystals can also be fabricated in colloidal systems using external fields such as holography¹⁰ or laser beams.¹¹

Quasicrystalline behavior arises due to the presence of two competing length scales, either induced by the different sizes of the two particle species in the case of binary mixtures, or due to an effective pair interaction that favors two length scales.¹² This leads to a broad classification of soft-matter quasicrystals into two categories: (1) binary mixtures, for example, of nanoparticles interacting with simple isotropic pair potentials, and (2) single-component systems, like micelles, with effective pair interactions that favor two length scales. Evidence of spontaneous formation of quasicrystalline order in soft-matter systems belonging to both categories have been observed in computer simulation studies. Examples of *in silico* quasicrystals in binary mixtures include particles interacting with Lennard-Jones^{13,14} and square-well¹⁵ potentials. Single-component quasicrystals have been observed in particles interacting with Lennard-Jones-Gauss,¹⁶ square-shoulder,¹⁷ square-well,¹⁸ linear ramp,¹⁹ flat-well,²⁰ and three-well oscillating²¹ pair interactions. For completeness, we mention that quasicrystals are also studied in systems of patchy particles and hard non-spherical particles such as tetrahedra²² and (truncated)

triangular bipyramids,^{23,24} where the interactions or particle shape generate local arrangements or packings that are compatible with quasicrystals.

From a theoretical point of view, the thermodynamic stability of these soft-matter quasicrystals is widely debated in the literature.^{25–27} The presence of two length scales in a single component system creates a core-corona type structure that is thought to stabilise the quasicrystal by reducing its surface area.^{28,29} Indeed, many experimentally discovered soft-matter quasicrystals in one-component systems frequently consist of spherical particles with a rigid core and a squishy corona, e.g., the spherical dendrite micelles consist of a rigid aromatic core with a deformable shell of alkyl chains,² and the block copolymer micelles consist of a micellar core of hydrophobic polymer surrounded by a large shell of hydrophilic polymer blocks.⁷ In addition, it was found by simulations that the mobility of the surface entities and shape polydispersity in the case of one-component micellar systems play an important role in the stabilisation of quasicrystals.³⁰ It is tempting to speculate that the role of the surface entities with respect to mobility and polydispersity is replaced by the smaller species in the case of quasicrystals of binary systems.

In order to prove the thermodynamic stability of quasicrystals, one has to show that the quasicrystal corresponds to the lowest free-energy state of the system. Quasicrystals can be either energetically or entropically stabilised.²⁵ An energetically stabilised quasicrystal results when the quasicrystal is the minimum-energy configuration at zero temperature.²⁶ On the other hand, when the configurational entropy outweighs the energetic contribution, the quasicrystal may be entropically stabilised at finite temperatures.²⁷

An extension of this debate deals with the relative stability of a random-tiling quasicrystal and its crystalline approximant at finite temperatures. A crystalline approximant is a periodic quasicrystalline counterpart which is described by a large unit

^{a)}h.pattabhiraman@uu.nl

^{b)}m.dijkstra@uu.nl

cell with a structure that resembles that of a quasicrystal.^{23,31} While the enthalpic and vibrational contributions to the free energy are assumed to be very similar for the quasicrystal and its approximant, the free energy of a random-tiling quasicrystal involves a configurational entropy contribution due to the number of distinct configurations,³² which is absent for the approximant.³³ We thus expect that the quasicrystal is more stable than the approximant due to its configurational entropy. On the other hand, one might expect the approximant to be more stable as it is assumed to have a lower energy and is considered to pack more efficiently due to the absence of defects.^{22,23,30} Hence, we conclude that it is still unresolved whether or not the quasicrystal is more stable than its crystalline approximant, and how this depends on the thermodynamic state of the system.

A major setback in determining the stability of these quasicrystals arises from the fact that computing their free energies is not straightforward. A reference state with known free energy from which thermodynamic integration can be performed to a quasicrystal is unknown. This issue is further complicated by the fact that there is no simple way to sample over the distinct configurations of the quasicrystal and to account for its configurational entropy.³² Recently, a method was proposed to determine the free energy of a quasicrystal by simulating the direct coexistence of a fluid and quasicrystalline phases of patchy particles.³³ Due to the lack of hysteresis in the fluid to quasicrystal transformation of this system, the free energy could be directly determined from the free energy of the fluid phase.

In this work, we follow a different route to determine the free energy of a two-dimensional random-tiling quasicrystal in a 2D system of hard disks interacting with a square-shoulder potential. We determine the free energy of a defect-free random-tiling quasicrystal and some of its approximants using thermodynamic integration to a non-interacting Einstein crystal.³⁴ We find that the free energy of the random-tiling quasicrystal is slightly lower than that of the crystalline approximants. For the random-tiling quasicrystal, we explicitly account for the configurational entropy using an expression from the literature.³⁵ Here, we approximate the configurational entropy by assuming that all possible realizations that are equivalent in the random-tiling model are also equally probable in our system. Finally, we also map out the phase diagram of the system under study and find that the defect-free random-tiling quasicrystal is stable with respect to the crystalline approximants that we considered, both with and without the additional configurational entropy term.

II. MODEL

In this paper, we focus on quasicrystalline order in one-component systems. We consider a 2D system of spherical particles decorated with a soft deformable corona mimicking the floppy corona of alkyl chains in the case of micellar particles or the squishy hydrophilic shell of block copolymer micelles. Analogous to previous work,¹⁷ we model this system by 2D hard disks with diameter σ interacting with a repulsive square-shoulder potential. Hence, the resulting pair potential of this hard-core square shoulder (HCSS) system reads

$$V_{HCSS}(r) = \begin{cases} \infty, & r \leq \sigma \\ \epsilon, & \sigma < r < \delta\sigma \\ 0, & r \geq \delta\sigma \end{cases}, \quad (1)$$

where r is the center-of-mass distance between two particles, and δ and ϵ are the square shoulder width and height, respectively. Despite the simplicity of the pair interaction, a whole family of quasicrystals with 10-, 12-, 18-, and 24-fold bond orientational order has been observed in a previous simulation study depending on the shoulder width-to-core ratio and the packing fraction.¹⁷ Here, we focus on a shoulder width $\delta = 1.4$, which gives rise to a dodecagonal quasicrystal at sufficiently low temperatures and high enough densities.¹⁷ At these conditions of shoulder width, temperatures, and densities, the system prefers the formation of square environments with four nearest neighbours to that of six coordinated hexagonal environments, thereby lowering its potential energy.

III. SIMULATIONS AND RESULTS

We perform Monte Carlo (MC) simulations in the canonical (NVT) and isothermal-isobaric (NPT) ensemble, where we fix the number of particles N , the temperature T , and the volume V or the pressure P , respectively. We employ a rectangular box of area A and apply periodic boundary conditions. We find that a random-tiling quasicrystal is formed either by compressing the fluid phase at a constant temperature or by cooling the hexagonal phase to a lower temperature at a constant density. In Fig. 1(a), we show a typical configuration of the quasicrystal for a system of $N = 4900$ particles as obtained at $\delta = 1.4$, $\rho^* = N\sigma^2/A = 0.98$, and $T^* = k_B T/\epsilon = 0.278$, where k_B is the Boltzmann's constant. In order to eliminate any effect of defects on the subsequent free-energy calculations, we constructed a defect-free random square-triangle tiling QC adapted from a non-Stampfli-type square-triangle approximant³⁶ which is shown in Fig. 1(b).

A significant fraction of local particle environments in dodecagonal quasicrystals has a coordination number of five. Depending on the local arrangement of squares and triangles around the central particle, these environments can be categorised as H or σ phases in analogy to the Frank-Kasper phases.³⁷ Both these phases can be considered as crystalline approximants to the dodecagonal quasicrystals. We term these as first-order crystalline approximants and their structures and corresponding diffraction patterns are shown in Figs. 1(c) and 1(d). It can be noted from the diffraction patterns that the H phase shows more linear order than the required dodecagonal symmetry, while the dodecagonal symmetry obtained in the σ phase is somewhat distorted. This is attributed to the low number of particles in the approximant unit cell, namely, 8 and 32 in the H and σ phases, respectively.

For further analysis, we construct second-order crystalline approximants with a larger number of particles in their unit cells. These consist of dodecagonal motifs of particles arranged either in a triangle (AC-tr)^{33,37} or a square-triangle (AC-sqr)³⁶ tiling, constituting 52 and 56 particles, respectively, in their unit cells. The latter was obtained by repeated vertex substitution of the (3².4.3.4) Archimedean tiling consisting

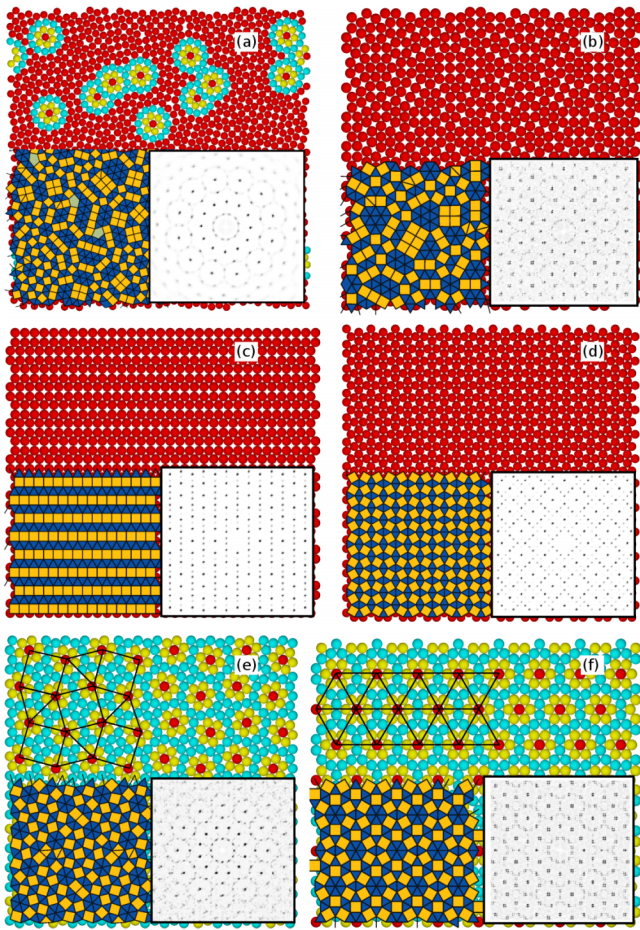


FIG. 1. Comparison of the quasicrystal and its crystalline approximants. Random tiling dodecagonal quasicrystal (QC), (a) as obtained from simulations, (b) defect-free configuration, (c) H phase, (d) σ phase and approximant crystals consisting of dodecagons in (e) square-triangle (AC-sqtr), and (f) triangle (AC-tr) tiling. (Top) Examples of a typical particle configuration showing dodecagonal arrangement of particles, if present. The tiling of the centers of dodecagons (marked red) is shown in ((e) and (f)). (Bottom) The corresponding square-triangle tiling (left) and diffraction pattern (right).

of squares and triangles.³⁸ These structures are shown in Figs. 1(e) and 1(f). It is good to mention that the AC-tr consists solely of σ environments, while the AC-sqtr consists of both H and σ environments.

To study the relative stability of the above mentioned phases, we first compare their equations of state, i.e., the pressure P as a function of density ρ , measured by varying the pressure in a step-wise manner in the NPT ensemble. We perform compression runs starting from a disordered fluid phase (FL), and expansion runs using a crystal phase with a square (SQ) or a hexagonal (HDH) symmetry, a defect-free random-tiling QC or either of its crystalline approximants (H , σ , AC-sqtr, or AC-tr). We plot the results for $T^* = 0.10$ in Fig. 2(a). Two essential observations can be made from these plots, namely, (1) the first-order approximants are less dense than the QC and the second-order approximants, which are all equally dense for all pressures higher than the melting point, and (2) the first-order approximants melt before the second-order approximants and the quasicrystal. This hints towards lower thermodynamic stability of the first-order approximants, namely, the H and σ phases, in comparison to the others.

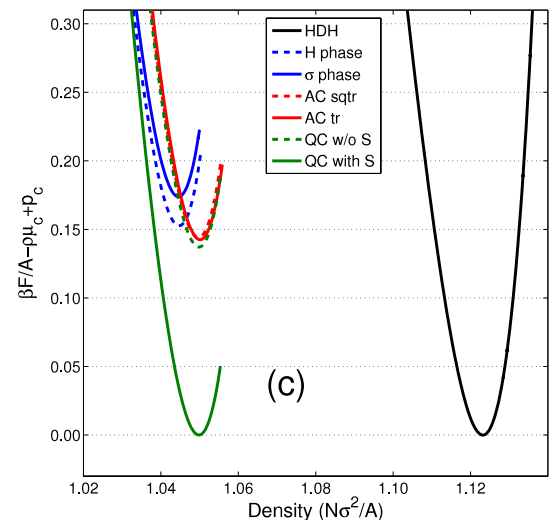
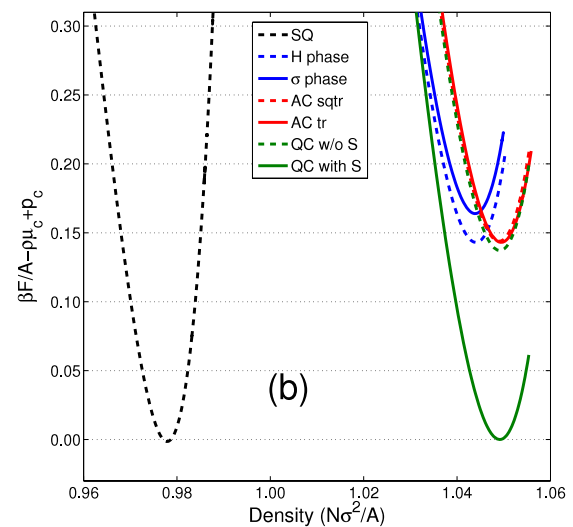
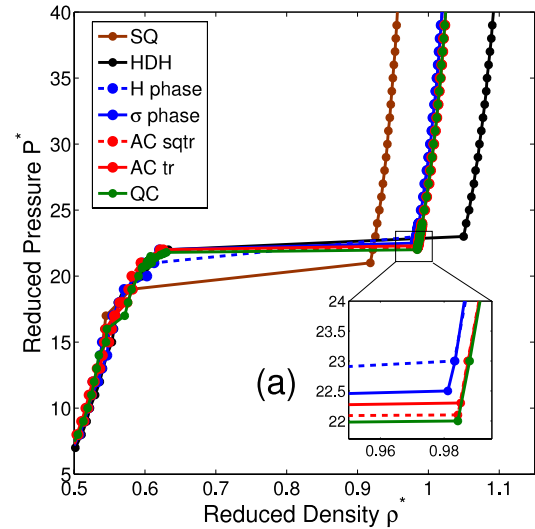


FIG. 2. Relative stability of the solid phases, namely, square (SQ), high-density hexagonal (HDH), quasicrystal (QC), H phase, σ phase and the two approximant crystals in square-triangle (AC sqtr) and triangle (AC tr) tiling at reduced temperature $T^* = k_B T / \epsilon = 0.10$ for a HCSS system with $\delta = 1.4$. (a) Equations of state, reduced pressure $P^* = \beta P \sigma^2$ versus reduced density $\rho^* = N \sigma^2 / A$. Common tangent construction at the (b) square-quasicrystal and (c) quasicrystal-high-density hexagonal phase coexistence, where we plot the Helmholtz free energy per area $\beta F / A$ as a function of reduced density ρ^* . For convenience, we subtract a linear fit $\rho \mu_c - p_c$, where μ_c and p_c are the bulk chemical potential and bulk pressure, respectively.

In order to identify the stable phases and the various phase transitions, we calculate the Helmholtz free energy F of the phases involved. We determine the free energy of the fluid phase by constructing a reversible path from the HCSS system to the hard-disk fluid at the same density,^{34,39} where we employ the free-energy expression for the hard-disk fluid by Santos *et al.*⁴⁰ For the crystalline phases, the free energy is calculated using the Frenkel-Ladd method by using the Einstein crystal as the reference state.^{34,41} Subsequently, we determine the Helmholtz free energy $F(\rho)$ of both the fluid and crystal phases by using thermodynamic integration of the equation of state $P(\rho)$.

Calculating the free energy of a quasicrystal is less trivial. This is because integrating from the fluid or ideal gas would involve crossing an intervening phase transition and on the other hand, using the Einstein crystal as a reference state in the thermodynamic integration would not account for the configurational entropy of the system. Also, in our system of particles, we do not observe a clear two-phase coexistence of the quasicrystal with another phase, viz., FL, SQ, or HDH, due to their structural similarities. In this work, we calculate the free energy of the quasicrystal using the Frenkel-Ladd method,³⁴ and subsequently add an additional configurational entropy contribution associated with the number of distinct random-tiling configurations.

An estimate for the configurational entropy for the dodecagonal quasicrystal has previously been obtained by numerically solving the Bethe ansatz for the square-triangle random tiling model.^{35,42,43} The maximum-entropy random tiling that results in a dodecagonal quasicrystal is observed at equal area fractions of squares and triangles,^{17,35} for which a value of $S_{\text{config}}/k_B A = 0.12934$ was obtained by Widom.³⁵ Indeed, the quasicrystals as obtained from our simulations exhibit a triangle area fraction of 0.50 ± 0.02 in good agreement with the maximum-entropy random tiling. It is good to point out that this value of configurational entropy considers a perfect random tiling of squares and triangles, where all configurations of the square and triangular tiles are equally probable. However, these tilings are not necessarily equivalent in our HCSS system, and the probability to find a certain tiling in our system should depend on its potential energy and its vibrational entropy. Therefore, the value used here is only an upper bound for the configurational entropy of the HCSS system.

Further, we construct common tangents between various sets of phases as a function of density to identify the most stable phase with dodecagonal symmetry and the various solid-solid phase transitions. To construct the common tangent, we plot the Helmholtz free energy per unit area $\beta F/A$ as a function of reduced density ρ^* , wherein we subtract a linear fit $\rho\mu_c - p_c$ with μ_c the bulk chemical potential of the coexisting phases and p_c the bulk pressure. The common tangent constructions between the quasicrystal with entropy correction and the square and hexagonal phases at $T^* = 0.10$ are shown in Figs. 2(b) and 2(c), respectively. The free energy of the defect-free QC with and without the configurational entropy correction is denoted by the solid and dashed green lines, respectively. From these common tangent constructions, we can conclude that the quasicrystal is the most stable dodecagonal symmetric phase under these conditions. Surprisingly, we

find that the random-tiling quasicrystal is even stable without the configurational entropy correction with respect to the various crystalline approximants within the statistical accuracy of our calculations. The lower free energy of the quasicrystal compared to its approximants, even without the configurational entropy correction, points at an (vibrational) entropic stabilisation of the quasicrystal. The vibrational entropy is related to the number of configurations that particles can explore while moving around their lattice positions. It is important to stress that the vibrational entropy is fully captured by our free-energy calculations, where the mean square displacements of the particles around their lattice sites are integrated as a function of the spring constant of the springs with which the particles are tied to their respective lattice positions.³⁴ We wish to remark here that the role of vibrational entropy is often not taken into account in the discussions regarding entropy versus energy stabilisation of quasicrystals. However, its role has been studied in the context of aperiodically modulated superstructures⁴⁴ and patchy particles.⁴⁵

For all temperatures considered in this study ($T^* \geq 0.05$), we find that the QC, even without the configurational entropy correction, is thermodynamically more stable than its approximants. Previous studies have reported a quasicrystal-approximant transition for a random-tiling quasicrystal at lower temperatures.³² On the other hand, the conjecture by Dotera *et al.*¹⁷ suggests the formation of a stable random-tiling dodecagonal quasicrystal at 0 K with a density $\rho^* \approx 1.07$ and ground state energy $E/\epsilon N$ of 2.536. We find that the closed packed density of the quasicrystal and the second-order approximants is indeed $\rho^* = 1.07$ with a potential energy $U = E/\epsilon N$ equal to 2.536 ± 0.002 . Extrapolating to lower temperatures, we speculate that the quasicrystal remains more stable than its approximants at finite temperatures. At zero temperature, the quasicrystal and the second-order approximants may be equally probable, considering their equal potential energy within our error bars.

The transformation from the square to the hexagonal phase can be essentially described by an increase in the triangle-to-square ratio upon increasing the density of the system. In other words, we find that the triangle-to-square ratio increases with density until it matches with the maximum entropy random tiling consisting of equal area fractions of squares and triangles. We then find the formation of a dodecagonal quasicrystal with a triangle-to-square ratio of $4/\sqrt{3} \approx 2.309$. It is interesting to note that the triangle-to-square ratio of the second-order approximants is 2.3, whereas that of the first-order approximants is equal to 2.0. The first-order approximants with a lower triangle-to-square ratio are thus formed at a density in between that of the square phase and the random-tiling quasicrystal phase as can also be seen in Fig. 2(a), and have a higher free energy than the quasicrystal as shown in Fig. 2(b).

In addition, we map out the phase diagram for this HCSS system with a shoulder width $\delta = 1.4$ using the common tangent construction to obtain the coexistence points. The resulting phase diagram is given in Fig. 3 in the (reduced) pressure-temperature and temperature-density planes. The stable phases identified in the system are the FL, SQ, low-density hexagonal (LDH), high-density hexagonal (HDH) phase, and the QC. We note that the quasicrystal is the thermodynamically

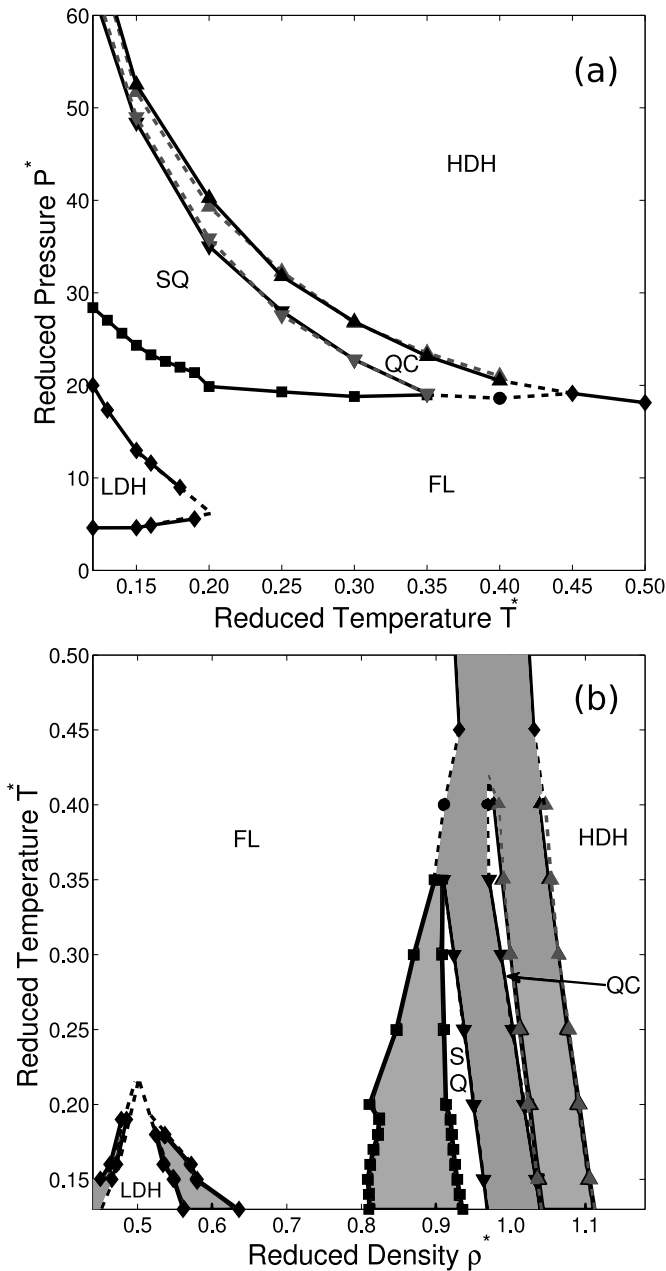


FIG. 3. Phase diagram of a two-dimensional hard-core square-shoulder (HCSS) system with a shoulder width $\delta = 1.4$ in the (a) pressure-temperature and (b) temperature-density planes. All quantities are represented in reduced units as $P^* = \beta P \sigma^2$, $T^* = k_B T / \epsilon$, and $\rho^* = N \sigma^2 / A$. The phases represented are fluid (FL), square (SQ), low-density hexagonal (LDH), high-density hexagonal (HDH) solids, and random-tiling quasicrystal (QC). The phase boundaries of the QC without the entropy correction, that accounts for the number of distinct configurations, are shown with dashed grey lines.

stable dodecagonal symmetric phase in the system and is stable over a range of temperatures ($0.10 \leq T^* < 0.45$) even without the configurational entropy term associated with the number of distinct configurations. The phase boundaries of the QC calculated without the additional configurational entropy correction are also shown with dashed grey lines. At lower temperatures ($T^* < 0.20$) and densities ($0.45 < \rho^* < 0.60$), we observe a re-entrant behavior of the fluid phase with a stable LDH phase region in between. The LDH phase is a consequence of the

repulsive square shoulder, which stabilizes a hexagonal phase with a lattice spacing of the order of the square shoulder width. At higher temperatures, $T^* \geq 0.45$, the phase behaviour of the system is similar to that of hard disks, with a fluid phase at low densities and a hexagonal phase at higher densities and a fluid-solid coexistence region in between. Given the system sizes used in this study, the presence of the hexatic phase is not considered.^{46,47}

IV. CONCLUSION

In conclusion, we investigated the phase behaviour of a model system of colloidal particles with a core-corona architecture. The particles are modeled by a hard-core square-shoulder pair potential with a shoulder width $\delta = 1.4$. We calculate the free energy of random-tiling quasicrystals by explicitly accounting for its configurational entropy. For this system, we find a stable quasicrystal region sandwiched between the high-density hexagonal phase and a square (fluid) phase at sufficiently low (high) temperatures. We confirm that the quasicrystal is stabilised over the crystalline approximants by its vibrational entropy. In future work, it is interesting to extend this study to different values of the shoulder width, which enables us to stabilize quasicrystals with 10-, 18-, and 24-fold bond orientational order,¹⁷ different particle potentials that may be more realistic, or to binary quasicrystals. Work along these lines is in progress.

ACKNOWLEDGMENTS

This work is part of the Industrial Partnership Programme “Computational Sciences for Energy Research” (Grant No. 12CSER004) of the Foundation for Fundamental Research on Matter (FOM), which is part of the Netherlands Organisation for Scientific Research (NWO). This research programme is co-financed by Shell Global Solutions International B.V. H.P. thanks G. Avvisati and J. R. Edison for helpful discussions and J. W. Burlage for initial work on this project.

¹D. Shechtman and I. Blech, *Phys. Rev. Lett.* **53**, 1951 (1984).

²X. Zeng, G. Ungar, Y. Liu, V. Percec, A. E. Dulcey, and J. K. Hobbs, *Nature* **428**, 157 (2004).

³A. Takano, W. Kawashima, A. Noro, Y. Isono, N. Tanaka, T. Dotera, and Y. Matsushita, *J. Polym. Sci., Part B: Polym. Phys.* **43**, 2427 (2005).

⁴T. Dotera and T. Gemma, *Philos. Mag.* **86**, 1085 (2006).

⁵K. Hayashida, T. Dotera, A. Takano, and Y. Matsushita, *Phys. Rev. Lett.* **98**, 195502 (2007).

⁶S. Lee, M. J. Bluemle, and F. S. Bates, *Science* **330**, 349 (2010).

⁷S. Fischer and A. Exner, *Proc. Natl. Aca. Sci. U. S. A.* **108**, 1810 (2011).

⁸D. V. Talapin, E. V. Shevchenko, M. I. Bodnarchuk, X. Ye, J. Chen, and C. B. Murray, *Nature* **461**, 964 (2009).

⁹M. I. Bodnarchuk, R. Erni, F. Krumeich, and M. V. Kovalenko, *Nano Lett.* **13**, 1699 (2013).

¹⁰Y. Roichman and D. Grier, *Opt. Express* **13**, 5434 (2005).

¹¹J. Mikhael, J. Roth, L. Helden, and C. Bechinger, *Nature* **454**, 501 (2008).

¹²T. Dotera, *Isr. J. Chem.* **51**, 1197 (2011).

¹³P. W. Leung, C. L. Henley, and G. V. Chester, *Phys. Rev. B* **39**, 446 (1989).

¹⁴K. J. Strandburg, *Phys. Rev. B* **40**, 6071 (1989).

¹⁵D. Salgado-blanco and C. I. Mendoza, *Soft Matter* **11**, 889 (2015).

¹⁶M. Engel and H. Trebin, *Phys. Rev. Lett.* **98**, 225505 (2007).

¹⁷T. Dotera, T. Oshiro, and P. Zihlerl, *Nature* **506**, 208 (2014).

¹⁸A. Skibinsky, S. V. Buldyrev, A. Scala, S. Havlin, and H. E. Stanley, *Phys. Rev. E* **60**, 2664 (1999).

¹⁹E. A. Jagla, *Phys. Rev. E* **58**, 1478 (1998).

- ²⁰L. Q. Costa Campos, C. C. de Souza Silva, and S. W. S. Apolinario, *Phys. Rev. E* **86**, 051402 (2012).
- ²¹M. Engel, P. F. Damasceno, C. L. Phillips, and S. C. Glotzer, *Nat. Mater.* **14**, 109 (2014).
- ²²A. Haji-Akbari, M. Engel, and S. C. Glotzer, *J. Chem. Phys.* **135**, 1 (2011).
- ²³A. Haji-Akbari, M. Engel, and S. C. Glotzer, *Phys. Rev. Lett.* **107**, 1 (2011).
- ²⁴A. Haji-Akbari, E. R. Chen, M. Engel, and S. C. Glotzer, *Phys. Rev. E* **88**, 1 (2013).
- ²⁵M. de Boissieu, *Philos. Mag.* **86**, 1115 (2006).
- ²⁶E. A. Jagla, *J. Chem. Phys.* **110**, 451 (1999).
- ²⁷K. Barkan, H. Diamant, and R. Lifshitz, *Phys. Rev. B* **83**, 172201 (2011).
- ²⁸P. Ziherl and R. D. Kamien, *Phys. Rev. Lett.* **85**, 3528 (2000).
- ²⁹P. Ziherl and R. D. Kamien, *J. Phys. Chem. B* **105**, 10147 (2001).
- ³⁰C. R. Iacovella, A. S. Keys, and S. C. Glotzer, *Proc. Natl. Acad. Sci. U. S. A.* **108**, 9 (2011).
- ³¹A. I. Goldman and R. F. Kelton, *Rev. Mod. Phys.* **65**, 213 (1993).
- ³²A. Kiselev, M. Engel, and H. R. Trebin, *Phys. Rev. Lett.* **109**, 1 (2012).
- ³³A. Reinhardt, F. Romano, and J. P. K. Doye, *Phys. Rev. Lett.* **110**, 255503 (2013).
- ³⁴D. Frenkel and B. Smit, *Understanding Molecular Simulation: From Algorithm to Applications* (Academic Press, 1996), ISBN: 0-12-267351-4.
- ³⁵M. Widom, *Phys. Rev. Lett.* **70**, 2094 (1993).
- ³⁶M. Oxborrow and C. L. Henley, *Phys. Rev. B* **48**, 6966 (1993).
- ³⁷M. N. van der Linden, J. P. K. Doye, and A. A. Louis, *J. Chem. Phys.* **136**, 54904 (2012).
- ³⁸M. O'Keeffe and M. M. J. Treacy, *Acta Crystallogr., Sect. A: Found. Crystallogr.* **66**, 5 (2010).
- ³⁹C. Vega and E. Sanz, *J. Phys.: Condens. Matter* **20**, 153101 (2008).
- ⁴⁰A. Santos, M. Lopez de Haro, and S. Bravo Yuste, *J. Chem. Phys.* **103**, 4622 (1995).
- ⁴¹J. M. Polson, E. Trizac, S. Pronk, and D. Frenkel, *J. Chem. Phys.* **112**, 5339 (2000).
- ⁴²W. Li, H. Park, and M. Widom, *J. Stat. Phys.* **66**, 1 (1992).
- ⁴³B. Nienhuis, *Phys. Rep.* **301**, 271 (1998).
- ⁴⁴M. Engel, *Phys. Rev. Lett.* **106**, 169901 (2011).
- ⁴⁵F. Smalenburg and F. Sciortino, *Nat. Phys.* **9**, 554–558 (2013).
- ⁴⁶E. P. Bernard and W. Krauth, *Phys. Rev. Lett.* **107**, 155704 (2011).
- ⁴⁷W. Qi, A. P. Gantapara, and M. Dijkstra, *Soft Matter* **10**, 5449 (2014).